EUROFUSION WPJET1-PR(16) 14768

S Mordijck et al.

Comparison of time-dependent ionization and density profile evolution of SOLPS-ITER simulations with JET experiments

Preprint of Paper to be submitted for publication in
22nd International Conference on Plasma Surface Interactions
in Controlled Fusion Devices (22nd PSI)

Comparison of time-dependent ionization and density profile evolution of SOLPS5.0 simulations with JET experiments

S. Mordijck[a], E.T. Meier[a], A. Salmi[b], T. Tala[b], A. Järvinen[c], L. Meneses[d], J. Svensson[e], R. Gomes[d], M. Maslov[f], JET contributors[g]

[a] *Dept of Computer Science, College of William and Mary, Williamsburg, VA 23187*
[b] *VTT Technical Research Centre of Finland, PO Box 1000, FI-02044 VTT, Espoo, Finland*
[c] *Lawrence Livermore National Laboratory, Livermore, CA 94550, USA*
[d] *Instituto de Plasmas e Fusão Nuclear, Lisbon, Portugal*
[e] *Max-Planck Institute for Plasma Physics, Greifswald, Germany*
[f] *CCFE, Culham Science Centre, Abingdon, OX14 3DB, UK*
[g] *EUROfusion Consortium, JET, Culham Science Centre, Abingdon, OX14 3DB, UK*

Abstract

The density profile at the plasma edge plays an important role in determining confinement properties, however little is known on what sets the profile shape. The difficulilty in examining the build of the density at the plasma edge lies in the impossibility to disentangle experimentally the different contributions of fueling, diffusion and particle pinch. To add to the complexity, the processes do not only vary radially but also poloidally. On the other hand, recent work with respect to ITER predictions shows gas fueling in L-mode has a limited effect upon the density, whereas in H-mode no limitation is observed, but the density pedestal completely disappears and $n_{ped} = n_{sep}$ [1]. In this paper, we will compare the time-dependent changes of the density with SOLPS5.0 as the result of a gas puff and compare these results directly to experimental observations made on JET. In our simulations, we will keep the transport coefficients fixed, as well as all the boundary conditions in order to just study the effect of an additional gas puff. We find that while the gas puff increases the density, the increase versus time in the simulation is slower than what is observed experimentally. Moreover, in the simulations the decrease of the density after the perturbative

---

Email address: `mordijck@cs.wm.edu` (S. Mordijck)

gas puff is removed, is on a faster time-scale than what is observed on JET. Both these observations, indicate that modeling particle transport using solely a diffusive component is not sufficient to capture the time-dependent changes and that we need to include an inward particle pinch inside the seperatrix. Prior experiments using a modulated gas puff have indicated the existance of a pinch [2, 3].

Keywords: fueling, particle transport, pedestal

---

1. Introduction

Our current understanding of what determines the density profile at the plasma edge is limited. There are theories that the density pedestal gradient is determined by the ionization source at the edge [4]. On the other hand, work on C-Mod has shown that changing the ionization source inside the seperatrix has no effect on the local density gradient [5]. Also, recent predictive simulations, using SOLPS, suggest that the high Srape-Off Layer (SOL) opacity will limit the ability to fuel the core plasma in L-mode [1]. In H-mode simulations for ITER, no such limitation is observed, however, due to the choice of only a diffusion coefficient, eventually $ne_{ped} = ne_{sep}$. These results completely counterdict the C-Mod experimental observations at high opacity [5].

The experimental results on C-Mod suggests that even if the ionization source is altered inside the seperatrix, transport self-adjusts itself to fit the critical-gradient model [5]. At the highest I_p values, which results in the highest SOL opacity, which strongly reduces the ability of the neutrals to penetrate inside the separatrix, no changes in the density were observed (not in the SOL and not in the pedestal). However, the experiments at low I_p and thus low SOL opacity show that the density increases everywhere by about the same amount when a gas puff is applied. This is in agreement with previous SOLPS simulations of H-mode plasmas on DIII-D, where changes in recycling and pumping efficiency did not change the local density gradient, but increased or lowered the density over the whole computational domain [6].

The assesment of neutral fueling versus transport for C-Mod was limited to a simple 1D neutral model and diffusive transport coefficients, however 2D fluid modeling has shown that fueling is not poloidally uniformly distributed on flux surfaces in a tokamak and that most of the fueling occurs at the X-point [7]. Moreover, while it is impossible to measure it directly, there is evidence through indirect measurements that particle transport is not purely diffusive, but that there is also a strong inward pinch in H-mode [2, 3, 8].

In this paper we will investigate how a short gas puff affects the density profile and neutral densities in a H-mode JET plasma. We use SOLPS5.0 and match the experimental conditions before the short 110 ms gas puff is applied. Next, we apply a gas puff in a time-dependent SOLPS simulation and compare the effects of the gas puff on the electron and neutral density after 70 and 110 ms. Finally, we compare the time dependent evolution of the SOLPS density calculation with the experimental observations. We find that while in the SOLP simulations, the density increases as a result of applying a gas puff, the density increase is too small inside the seperatrix when compared to experimental observations. Also, once the perturbative gas puff is removed in the simulations after 110 ms, the density reduces immediately in the simulations, whereas in the experiment, the density still remains at its maximum value for at least another 70 ms. Both these observations indicate that in the simulations, the fueling from the perturbative gas puff does not penetrate as well as in experiments, which might be an indication that we need an inward pinch to match the experimental observations. An inward pinch, would also slow down the density pump-out after the perturbative gas puff is removed.

2. Experimental conditions

We start from a set of dedicated experiments in JET where a gas puff modulation at a constant frequency is applied to a set of H-mode plasmas in which collisionality was varied dimensionlessly [8, 9]. In this paper, we will only use the discharge at the lowest collisionality, $\nu* = 0.1$ (discharge 87424). The plasma

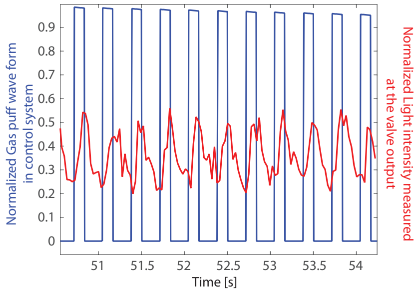

Figure 1: Normalized programed gas puff modulation in blue versus time for discharge 87424. In red is the normalized (versus the highest value during this time) of the light intensity measured with the fast camera at the valve entrance to the main chamber. There is a short time delay of about 20 ms between the programmed gas puff modulation and when the gas enters the vessle on JET for this valve.

current is $I_p = 2.5\ MA$ and the toroidal magnetic field is $B_T = 3.3\ T$, which results in a $q_{95} = 4$. The line averaged density is $5.1 \times 10^{19}\ m^{-3}$ and for our simulations we will assume $T_e = T_i$ at the plasma edge, which is a good estimate based on rough T_i measurements. The greenwald fraction is 0.65 and $\beta_N = 0.81$. These are H-mode plasmas and the ELM frequency is about 95 Hz, which is much faster than the frequency of the gas puff modulation of 3 Hz. These plasmas have a constant gas puff providing the fueling to maintain a constant density using an outlet just above the inner strike-point where the magnitude of the puff is 6×10^{21} electrons/s. On top of this steady-state fueling puff, we apply a modulated gas puff using a valve located close to the crown of the plasma, see figure 1. The frequency of the modulation is 3 Hz, where the gas puff is on for 1/3 of cycle and off for 2/3. This means, the gas puff is on for close to 110 ms and off for about 220 ms. During the on period, 6.5×10^{22} electron/s are injected. In figure 1, we can also observe that there is a time-delay between when the valve for the gas puff opens and when the gas appears at the top of the machine. The light intensity as measured with a fast camera, increases only between 20-50ms after the valve is opened. This means, that if we set $t = 0$ at the start of the valve opening in our modeling, that our results will be off by

20-50ms. As a result, we choose $t = 0$, 20 ms after the gas valve is opened in our simulations.

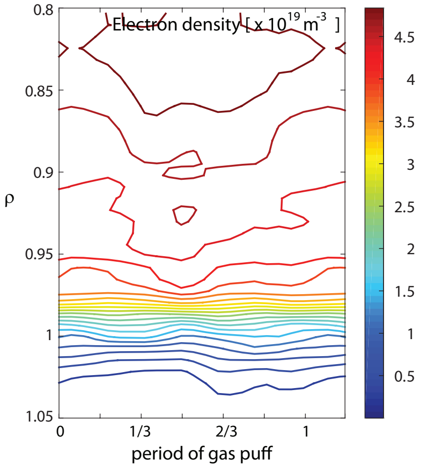

Figure 2: Compound Thomson Scattering data, averaged over the whole modulation period and fitted back to one single gas puff modulation period.

In order to investigate how the density profile is affected by this gas puff, we conditionally average the Thomson Scattering data over the 10 cycles of the modulation. This allows us, to increase our confidence that the observed changes in density are real and not an artifact a measurement error. The datapoint over the 10 cycles are mapped to 1 cycle, which increase the amount of datapoints at each time in 1 cycle, increasing the temporaral resolution, see figure 2. These profiles are aligned with the gas valve signal in figure 1 and not with the observation of when gas first enters the vessle. In order to account for this delay, we choose the density to which we fit our $t = 0$ SOLPS simulation 20 ms into this cycle.

3. SOLPS modeling

We use SOLPS5.0 to model the evolution of the density and the neutral concentration during the gas puff [10]. SOLPS5.0 is a code package which consists of two components: B2 [11], a 2D fluid plasma boundary code and EIRENE, a

Monte-Carlo neutral code [12]. Both codes are coupled and iteratively evolve the changes to the plasma and the neutrals by stepping forward in time. By making the time-steps and the amount of time-steps identical, we can use the code to make time-dependent simulations to study the effects of a gas puff. The grid goes up to $\rho \sim 0.8$ in the core and counts 30 cells in the radial direction (15 in the core and 15 in the SOL) and 120 cells poloidally, where 80 cover the core and the remaining 40 are split evenly between the inner and outer divertor. In the core we use fluxes as boundary conditions, with the particle flux $\Gamma_p = 1.0 \times 10^{20}\ 1/m^2 s$, the electron heat flux $\Gamma_e = 1.0 \times 10^5\ W/m^2$ and the ion heat flux, $\Gamma_i = 0.9 \times 10^5\ W/m^2$. At outer SOL boundary we use an exponential fall-off length set at 0.01 m for the density as well as the electron and ion temperatures. The interaction at the divertor plates is characterized by a Bohm-Chodura sheath boundary conditions and ad-hoc flux limitations for the heat fluxes. In EIRENE, all the recycling coefficients are set to 1, with exception of where the B2 grid interacts with the wall. There to match divertor density conditions as well as the fact that the strike-points are close to the pump entrances, we find that recycling coefficients of 0.9 result in a good match to experimental observations of the density in the divertor area. In these experiments, the outer strike-point is swept with a frequency of 4 Hz, this is another reason why we set the recycling to 0.9 over the whole computational domain of where B2 intersects with the wall, instead of only at the pump-entrance. Our modeling does not include the sweeping of the strike-point and we will thus look at the average values for divertor conditions. In EIRENE we also add the steady-state gas puff, at the same location as where the gas valve is located in the JET experiments above the inner strike-point and the magnitude is based on the magnitude determined from experiments. None of the simulations include drifts.

3.1. Before the gas puff

In order to match the plasma conditions to before the perturbative gas puff is applied, we alter the transport coefficients until we find a good match for the

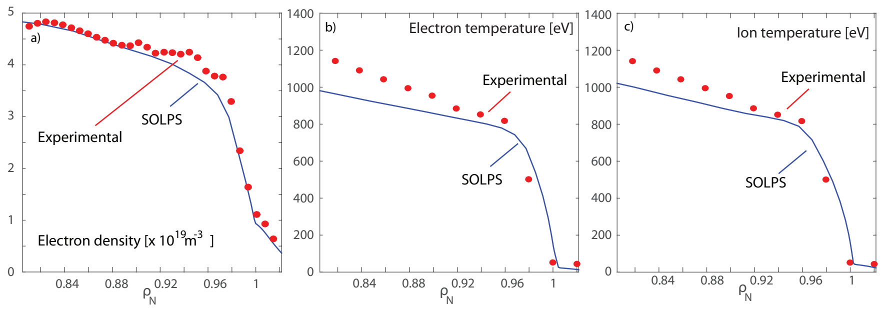

Figure 3: (a) Experimental electron density profile (red dots) versus SOLPS5.0 simulation (blue line) before the gas puff is applied to extract the transport coefficients. (b) A similar approach is taken for the electron temperature and the (c) and the ion temperature.

upstream simulations with experimental measurements along with the general conditions in the divertor area. It is important to get reasonably good matches to experimental conditions, in order to have similar ionization rates to those that occur in the experiment. Figure 3 shows the SOLPS simulated density and temperatures and how they compare to experimental values. From the experiment as mentioned before, we assume the ion temperatures are equal to the electron temperatures. All radial transport in these simulations is assumed to be diffusive. This is for simplicity, even if in reality particle transport needs to be split into a diffusion as well as convection coefficient. These conditions is the starting point to our time-dependent simulations in which we look at the effect of adding a gas puff.

3.2. During and after the gas puff

We add a gas puff, based on experimental values at the top of the JET vessle. In this section we compare the density evolution after 70 ms, 110 ms (the end of the gas puff) and 180 ms (70ms after the gas puff stops) with the experimental changes in density. We observe that the gas puff results in an increase in the core density, similar to what is observed experimentally. After 70 ms, the increase in density in the SOLPS simulation is similar over a wide radial extend to the experimental observations, see figure 4. The only place

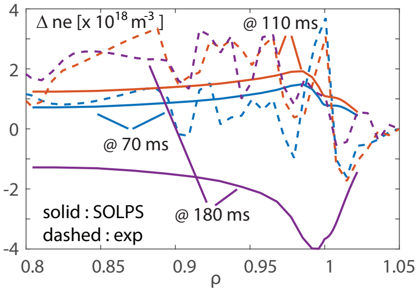

Figure 4: $\Delta n_e = n_{e_i} - n_{e_0}$, where n_{e_0} is the density before the gas puff is applied and n_{e_i} is the density at time i. The dashed lines are the experimental values and the solid lines are based on the SOLPS5.0 simulations.

where there is a large discrepancy between experimental observations and the SOLPS simulations is just inside the separatrix. Here the experiment shows a much larger increase in the density, in comparison with the SOLPS simulations. However, once we reach 110ms of gas puffing in the SOLPS simulations, the density increase in the SOLPS simulations is smaller over the whole computational extend, when compared to experimental observations. At the same time, we observe an increase in the outer divertor density to 6×10^{19}, which is much larger than measured experimentally and results in the onset of detachment of the outer leg in the simulations. Both these results, suggest that gas puff in the simulation is not as effective at fueling the plasma core. In the simulation we only use a diffusion coefficient for particle transport and this result is a first indication that there must a particle pinch at the plasma. This is confirmation of previous experimental work using a perturbative pinch in H-mode plasmas, that there is an inward particle pinch at the plasma edge.

Next, after puffing for 110ms in our simulation, we now turn off the perturbative gas puff at the top of the machine. Without changing boundary conditions or transport coefficient, we compare the evolution of the density profile. In figure 4, we can observe that 70ms after the gas puff is remove (after 180ms into the cycle), the density is strongly reduced. However, experimentally the density has not yet dropped from when the gas puff was removed at 110ms. This is a second indication, that while the diffusive transport did capture the steady-state conditions, before the gas puff modulation was applied, it does not capture the time-dependent evoluation of the density during this gas puff modulation experiments. This confirms that we will need to change the ratio of diffusion to pinch in our simulations.

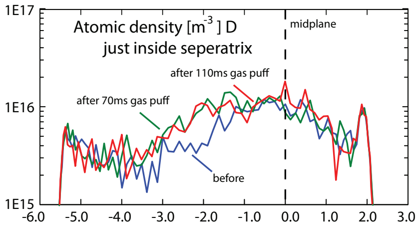

Figure 5: Changes in the polodial neutral density distribuation during the gas puff modulation. The largest increase in neutral density is close to the top of the machine and the increase in neutral density has saturated by the time the simulation reaches 70 ms.

To get a better idea of how fueling changes during this evolution, we compare the poloidal distribution of the neutral density just inside the separatrix in our simulations. We find that the gas puff at the top of the machine, mostly increases the neutral density at the top of the plasma just inside the separatrix, see figure 5. We also observe that the neutral density does not change from 70ms to 110ms into the simulation. Indicating that the increase in neutral fueling is fairly instantenous and saturates.

4. Discussion and Conclusion

In this paper, we use SOLPS to model the time-dependent evoluation of a gas puff and compare these results directly to experimental observations on JET. We start from matching most experimental parameters and only using diffusive transport coefficients. We find that using diffusive transport coefficients results in an underestimate of the density rise that is observed experimentally and a too large decrease of the density after the gas puff is turned off. This indicates that over this 'long' period, on average an inward pinch is needed to capture the time-dependent evoluation. We use the term "average", since the SOLPS calculations do not include the time-dependent transport changes as a result of Edge Localized Modes (ELMs) that are a standard feature of H-mode discharges [13].

ELMs do not only reduce the temperatures at the plasma edge, but also the density. The density rebuilds after an ELM crash, without an increase in core fueling. It is difficult to assess how ELMs affect 'average' transport, but the build of the density after an ELM crash is thought to be the result of an inward pinch. With ELMs being a regular and period feature of the pedestal in H-mode, our mode is interested in the average transport, over a large set of ELMs, not in the dynamics of the ELM itself. Experimentally, the gas puff increases the frequency of the ELMs, but at the same time, it decreases the size. So we assume in this paper it does not strongly affect the average particle flux.

Finally, we performed a sensitivity scan of the applied gas puff in our simulations, by increasing its magnitude by a factor 2 as well as reducing the magnitude of the puff by a factor 5. We find that when we increase the gas puff by a factor 2, we get a MARFE and a collapse of the core temperatures and density after only 10 ms. At the same time, when we reduce the perturbative gas puff by a factor 5, we observe an actual decrease in the core density. A careful analysis of this unusual feature is linked to the high neutral density blob that sits close to the inner leg, which has been observed on AUG and JET in recent years [14].

This work is a first step to using an edge modeling code like SOLPS to assess the time-dependent evolution of the density during a gas puff. The role of edge fueling versus an inward particle pinch is a current and important question that needs to be addressed in order to be able to make predictions for ITER and future machines. All current predictions for ITER rely on a purely diffusive particle transport at the plasma edge, which, based on experimental observations is incorrect.

In these experiments as well as in the simulations we ignore the effect the gas puff has on the ELM frequency. The ELM frequency increases slightly during the gas puff, but the size of the ELMs decreases. Analysis has shown that on average this increase in the ELM frequency does not increase the average particle transport. Another aspect is, that we assume that there is an 'average' transport accross ELMs. However, an ELM itself strongly perturbes the density profile and temperature profiles [15]. So transport in these ELMing H-mode plasmas, is not constant and varies before, during and after ELMs. We are at this point interested in the average transport accross multiple ELMs, but the pinch component could be much larger after an ELM crash to help rebuild the density profile and even become outward during the ELM crash itself. While the reflectometer might provide a high enough resolution during H-mode discharges without too high an ELM frequency to diagnose the changes in the density profile, the interplay of fueling and particle transport at the plasma edge, make it extremely difficult to extract any simple conclusions on how transport changes during one ELM cycle. As a result, we focus on understanding how transport at the plasma edge changes over multiple ELM cycles and we neglect the individual ELM dynamics.

Acknowledgement

This material is based upon work supported by the U.S. Department of Energy, Office of Science, Office of Fusion Energy Sciences under Awards DE-SC0007880 and DE-SC0010434.This work has been carried out within the framework of the EUROfusion Consortium and has received funding from the Euratom research and training programme 2014-2018 under grant agreement No 633053. The views and opinions expressed herein do not necessarily reflect those of the European Commission. This work was performed in part using the computational facilities at the College of William & Mary which were provided with the assistance of the National Science Foundation, the Virginia Port Authority, and Virginias Commonwealth Technology Research Fund.

5. Bibliography styles

References

[1] M. Romanelli, V. Parail, P. da Silva Aresta Belo, G. Corrigan, L. Garzotti, D. Harting, F. Koechl, E. Militello-Asp, R. Ambrosino, M. Cavinato, A. Kukushkin, A. Loarte, M. Mattei, R. Sartori, Nuclear Fusion 55 (2015) 093008. URL: `http://stacks.iop.org/0029-5515/55/i=9/a=093008`.

[2] S. Mordijck, E. J. Doyle, G. R. McKee, R. A. Moyer, T. L. Rhodes, L. Zeng, N. Commaux, M. E. Fenstermacher, K. W. Gentle, H. Reimerdes, O. Schmitz, W. M. Solomon, G. M. Staebler, G. Wang, Physics of Plasmas (1994-present) 19 (2012) –. doi:`http://dx.doi.org/10.1063/1.4718316`.

[3] S. Mordijck, T. Rhodes, L. Zeng, E. Doyle, L. S. C. Chrystal, T. Strait, R. Moyer, Effect of resonant magnetic perturbations on turbulence and transport in DIII-D L-mode plasmas, 2015. Submitted.

[4] R. Groebner, M. Mahdavi, A. Leonard, T. Osborne, N. Wolf, G. Porter, P. Stangeby, N. Brooks, R. Colchin, L. Owen, Nuclear Fusion 44 (2004) 204. URL: `http://stacks.iop.org/0029-5515/44/i=1/a=022`.

[5] J. Hughes, B. LaBombard, J. Terry, A. Hubbard, B. Lipschultz, Nuclear Fusion 47 (2007) 1057. URL: `http://stacks.iop.org/0029-5515/47/i=8/a=041`.

[6] S. Mordijck, et al., J. Nucl. Mat. 390-391 (2009).

[7] M. Groth, G. D. Porter, T. D. Rognlien, S. Wiesen, M. Wischmeier, M. N. A. Beurskens, X. Bonnin, B. D. Bray, S. Brezinsek, N. H. Brooks, D. P. Coster, T. Eich, M. E. Fenstermacher, C. Fuchs, R. A. Groebner, D. Harting, A. Huber, S. Jachmich, A. Kallenbach, C. J. Lasnier, A. W. Leonard, A. Meigs, H. W. Mller, M. E. Rensink, D. L. Rudakov, J. G. Watkins, E. Wolfrum, the DIII-D, ASDEX Upgrade Teams, J. Contributors, Plasma Physics and Controlled Fusion 53 (2011) 124017. URL: `http://stacks.iop.org/0741-3335/53/i=12/a=124017`.

[8] A. Salmi, T. Tala, P. Mantica, A. Jarvinen, L. Meneses, S. Mordijck, V. Naulin, J. J. Rasmussen, J. Svensson, L. Giacomelli, R. Gomes, M. Groth, T. Koskela, C. Maggi, M. Maslov, G. Sips, H. Weisen, JET contributors, in: 41st EPS Conference.

[9] T. Tala, P. Mantica, A. Salmi, C. Bourdelle, C. Giroud, J. Hillesheim, C. Maggi, L. Meneses, M. Maslov, S. Menmuir, S. Moradi, S. Mordijck, V. Naulin, H. Nordman, J. J. Rasmussen, G. Sips, A. Sirinelli, M. Tsalas, H. Weisen, JET contributors, in: 41st EPS Conference.

[10] R. Schneider, et al., Contr. plasma phys. 46 (2006).

[11] B. Braams, Computational studies in tokamak equilibrium and transport, Ph.D. thesis, Rijksuniversiteit Utrecht, 1986.

[12] D. Reiter, J. Nucl. Mat. 196-198 (1992).

[13] H. Zohm, Plasma Physics and Controlled Fusion 38 (1996) 105. URL: `http://stacks.iop.org/0741-3335/38/i=2/a=001`.

[14] S. Potzel, M. Wischmeier, M. Bernert, R. Dux, F. Reimold, A. Scarabosio, S. Brezinsek, M. Clever, A. Huber, A. Meigs, M. Stamp, Journal of Nuclear Materials 463 (2015) 541 – 545. doi:`http://dx.doi.org/10.1016/j.jnucmat.2014.12.008`.

[15] L. Zeng, G. Wang, E. Doyle, T. Rhodes, W. Peebles, M. Fenstermacher, T. Evans, R. Moyer, Journal of Nuclear Materials 337339 (2005) 742 – 746. doi:`http://dx.doi.org/10.1016/j.jnucmat.2004.09.037`.